Applied Catalysis B: Environmental 244 (2019) 215–224

Contents lists available at ScienceDirect

Applied Catalysis B: Environmental

journal homepage: www.elsevier.com/locate/apcatb

Electrocatalytic dechlorination of 2,4-dichlorobenzoic acid using different carbon-supported palladium moveable catalysts: Adsorption and dechlorination activity

Jiasheng Zhou[a], Zimo Lou[a,b], Kunlun Yang[a], Jiang Xu[b,*], Yizhou Li[a], Yuanli Liu[a], Shams Ali Baig[c], Xinhua Xu[a,*]

[a] Department of Environmental Engineering, College of Environmental and Resource Sciences, Zhejiang University, Hangzhou, 310058, People's Republic of China
[b] Department of Civil and Environmental Engineering, Carnegie Mellon University, Pittsburgh, PA, 15213, United States
[c] Department of Environmental Sciences, Abdul Wali Khan University, Mardan, 23200, Pakistan

ARTICLE INFO

Keywords:
2,4-Dichlorobenzoic acid
Carbon supported Pd catalyst
Electrocatalytic dechlorination
Adsorption
Stability

ABSTRACT

In the present study, carbon black (CB), multi walled carbon nanotubes (MWCNTs), and granular activated carbon (GAC) were employed to support palladium (Pd) catalyst. The prepared Pd/CB, Pd/MWCNTs and Pd/GAC moveable catalysts were aimed to address the common issues (easy loss of catalyst and poor long-term performance) of normal fixed catalysts. The results of various characterizations (e.g., TEM, XRD, and XPS) clearly show that the Pd nanoparticles were successfully loaded onto the carbon-supports, especially CB and MWCNTs. And more importantly, the morphologies, Pd distribution, and chemical structure of these moveable catalysts were almost not changed after 3 h reaction. The moveable Pd/CB, Pd/MWCNTs, and Pd/GAC catalysts had good reactivity for 2,4-dichlorobenzoic acid (2,4-DCBA) dechlorination, and Pd/CB exhibited the best performance. The Pd/CB also shows the best adsorption capacity of 2,4-DCBA and dechlorination product (benzoic acid, BA), and the adsorption of BA was significantly inhibited in the presence of current due to the repulsion between the both negatively charged compounds and adsorbents. The removal of 2,4-DCBA and the generation rate of BA was improved with a pre-adsorption process, which was a promising strategy with higher dechlorination rate and shortened electrolysis time. Moreover, the loss of Pd catalyst was negligible during the 10 consecutive cycles experiment, and the improved longevity could be expected. These results suggested the good reactivity, stability, and reusability of moveable Pd/CB catalyst.

1. Introduction

Various techniques including biological, thermal, and chemical treatments have been developed for the degradation of chlorinated organic compounds (COCs) [1,2]. Among these techniques, electrocatalytic reductive dechlorination has been considered as a promising water treatment strategy for the detoxification of COCs, and has attracted more attention in recent years [3–7]. Electrocatalytic reductive dechlorination can selectively remove chlorine atoms from chlorinated compounds under mild experimental conditions [8–10].

Generally, in the conventional electrocatalytic reductive methods for the dechlorination of COCs, catalysts are loaded on the fixed electrode plates [11–13]. But this method is reported to suffer from the desquamation problem, which resultantly declines reactivity, longevity, and recyclability of the catalytic electrode [14,15]. To overcome such issues, an electrode system that consisted of catalyst modified carriers and the fixed electrode plate has been proposed [16]. Carbon-based materials are widely used as the carriers of catalyst due to their large specific surface area [17–19]. These moveable catalysts can achieve high electrocatalytic efficiency and low energy consumption by providing numerous active sites and promoting the electro-generation of atomic H^* [20,21]. Also, the large surface area of the particle carriers can improve the dispersity of catalyst, enhance the mass transfer [22–26], and increase the adsorption capacity to COCs [27]. However, the effects of the carbon type on the distribution and reactivity of catalyst was still elusive, as well as the role of contaminant adsorption onto the catalyst in the electrocatalytic dechlorination.

Palladium (Pd) is a good and well-known catalyst, which plays an important role in the generation of atomic H^* for dechlorination [27–34]. Carbon black (CB), multi walled carbon nanotubes

* Corresponding authors.
E-mail addresses: jiangx2@andrew.cmu.edu (J. Xu), xuxinhua@zju.edu.cn (X. Xu).

https://doi.org/10.1016/j.apcatb.2018.11.052
Received 27 June 2018; Received in revised form 28 October 2018; Accepted 17 November 2018
Available online 20 November 2018
0926-3373/

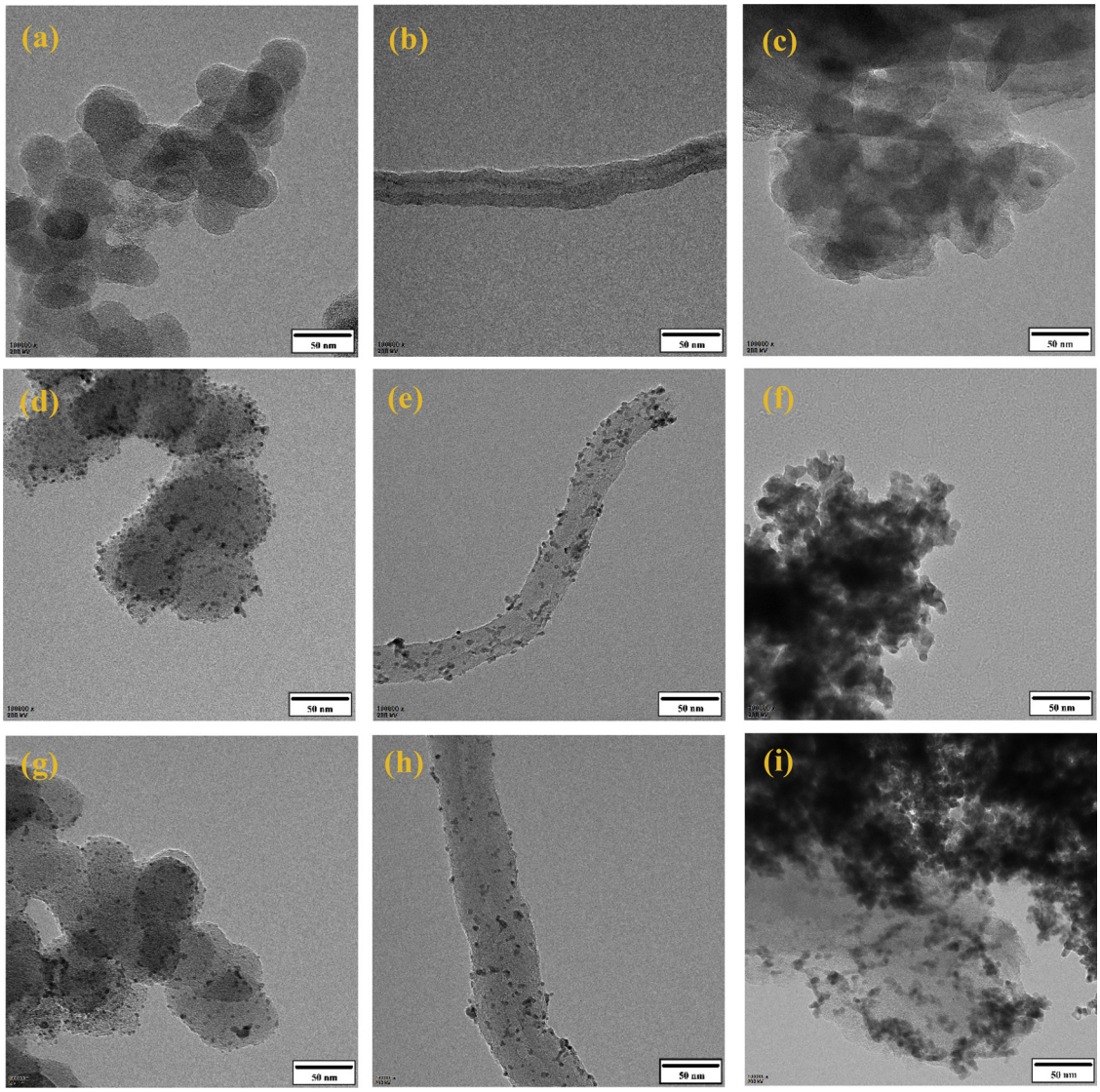

Fig. 1. TEM images of (a–c) bare CB, MWCNTs, and GAC; (d–f) Pd/CB, Pd/MWCNTs, and Pd/GAC before reaction; (f–i) Pd/CB, Pd/MWCNTs, and Pd/GAC after 3 h reaction.

(MWCNTs), and granular activated carbon (GAC) were chosen as the carbon-based carriers to support the Pd catalyst in this study. The reactivity of the moveable catalysts was investigated using 2, 4-dichlorobenzoic acid (2,4-DCBA) as a probe for chlorinated contaminants. 2,4-DCBA was selected as reactant due to its relatively non-volatility and aqueous solubility [35]. The effects of carbon types on the reactivity and distribution of Pd catalyst were investigated via batch experiments and various characterizations. The adsorption capacity of the contaminant on the carbon-supported Pd catalyst and the effect of the pre-adsorption on the dichlorination of 2,4-DCBA were studied, in order to understand the role of adsorption in the electrocatalytic dechlorination. Finally, consecutive experiments were performed to investigate the stability and reusability of the moveable catalyst.

2. Materials and methods

2.1. Materials

Nanoscale carbon black (CB) was purchased from Cabot Co, US. Multi walled carbon nanotubes (MWCNTs) were provided by Shenzhen Nanotech Port Co, Ltd, China. Granular activated Carbon (GAC) was obtained from a local company (Lishui City, Zhejiang Province, China). 2, 4-DCBA, and its intermediated products (o-chlorobenzoic acid and 4-chlorobenzoic acid, denoted as CBA in this study due to their low concentration in the reaction), and the final dechlorinated product (benzoic acid, BA) were purchased from Aladdin Reagent Inc., China. Nickel foam (Ni; pore density, 110 ppi; porosity, 99.8%; surface density, 380 g m^{-2}) was purchased from Kunshan Teng Erhui Electronic Technology Co., Ltd. Sodium citrate, sodium borohydride ($NaHB_4$), and sodium sulfate (Na_2SO_4) were obtained from Sinopharm Chemical Reagent Co., Ltd., China.

2.2. Preparation of Pd/CB, Pd/MWCNTs, and Pd/GAC

Pd/CB, Pd/MWCNTs, and Pd/GAC moveable catalysts were prepared via the reduction and deposition of Pd nanoparticles using a previous reported method [36–39]. Briefly, 1 mmol of K_2PdCl_6 and 8 mmol of sodium citrate were dissolved into 200 mL water, then 425.6 mg carbon (GAC, CB, and MWCNTs, respectively) were added and sonicated for 30 min to obtain an even suspension. 100 mL $NaBH_4$ solution (0.1 mM) was dropwise added into the suspension under vigorous stirring at 25 °C. Pd^{4+} was reduced and Pd nanoparticles were deposited onto the carbon supports after stirring for 4 h. The obtained Pd/CB, Pd/MWCNTs and Pd/GAC suspensions were filtered, and almost

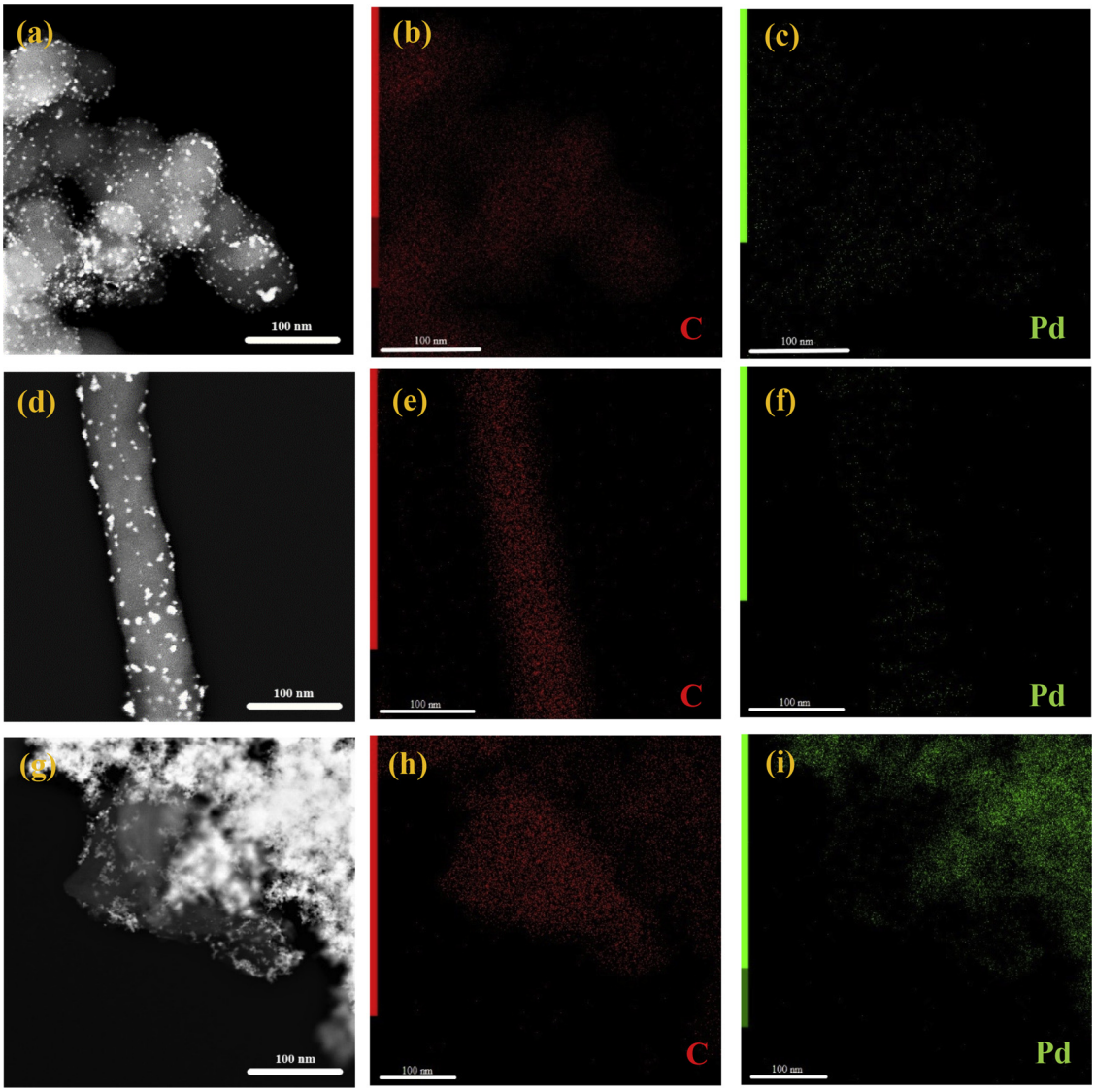

Fig. 2. TEM-EDS mapping images of (a–c) Pd/CB, (d–f) Pd/MWCNTs, and (f–i) Pd/GAC.

no Pd was detected by ICP-MS in the filtrate solution, suggested that almost all the Pd was deposited onto the carbon supports. The catalysts were thoroughly washed to remove impurities, and dried in a vacuum oven at 60 °C for 12 h.

2.3. Electrocatalytic dechlorination experiments

Electrocatalytic dechlorination of 2,4-DCBA by Pd/CB, Pd/MWCNTs, and Pd/GAC moveable catalysts were carried out in a two-compartment cell reactor. A cation-exchange membrane (Nafion 117) was used to separate the anode cell and cathode cell to reduce the negative impact of oxygen produced on the anode. It also prevents chloride ions produced at cathode cell from generating Cl_2 in the anode cell [40]. The electrocatalytic dechlorination reactions were performed by an SK1760SL20 A direct-current supply source at constant current. Based on our preliminary test, 2,4-DCBA was almost not be removed under 5 mA in the 3 h reaction, and could be efficiently removed under 10 mA and 15 mA. From the energy consumption point of view, 10 mA was selected as the constant current to study the performance of different carbon supported Pd catalysts in this study.

Ni foams (20 mm × 30 mm × 1.5 mm) and Platinum (Pt, 20 mm × 30 mm × 1 mm) were used as cathode electrode substrate and anode electrode substrate, respectively. For each electrocatalytic dechlorination experiment, 100 mL solution contained 10 mM Na_2SO_4 and 0.156 mM 2, 4-DCBA was added into the cathode cell (located in a 30 °C water bath), and 100 mL solution of 10 mM Na_2SO_4 was added into the anode cell correspondingly. Then, 40 mg of catalyst (contained 8 mg of Pd) was added into the solution and connected to the electric circuit. A constant speed magnetic stir bar was placed in the cathode compartment to eliminate the effect of concentration polarization. At different set times, a 0.5 mL sample was withdrawn from the cathode compartment for further analysis.

2.4. Adsorption capacities of different moveable catalysts for 2,4-DCBA and BA

The adsorption capacities of Pd/CB, Pd/MWCNTs, and Pd/GAC towards 2,4-DCBA and BA were carried out in the same two-compartment cell reactor. Each adsorption experiment was performed in the cathode cell with 100 mL solution contained 10 mM Na_2SO_4 and 0.156 mM 2, 4-DCBA or BA. Then, 40 mg of catalyst (contained 8 mg of Pd) was added into the cathode cell. Other conditions were also the same as the dechlorination experiment, except the current. The adsorption of 2,4-DCBA was performed without current (10 mA), and the adsorption of BA was performed with or without current, respectively.

Pre-adsorption experiment was performed via adding the catalyst

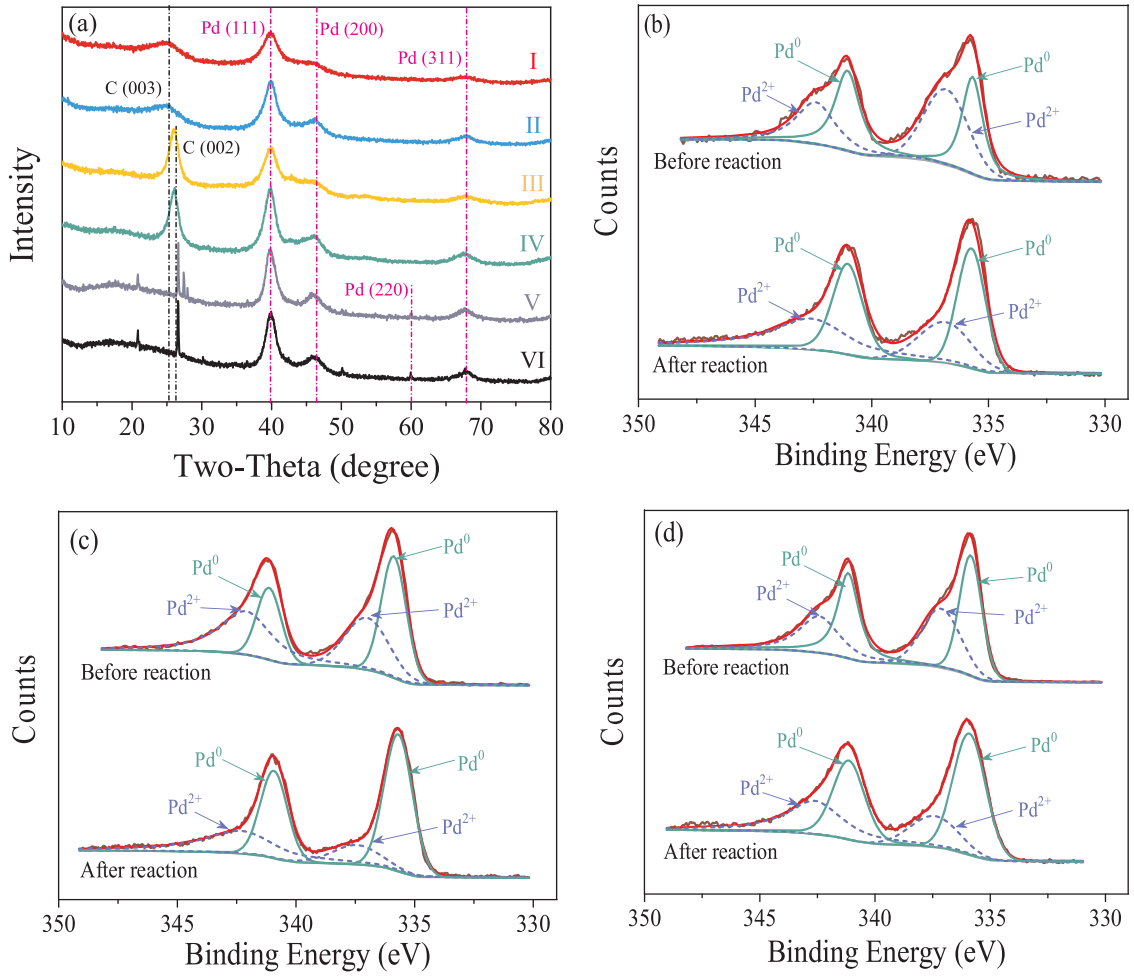

Fig. 3. (a) XRD patterns of Pd/CB (curves I and II), Pd/MWCNTs (curves III and IV), and Pd/GAC (curves V and VI) before and after 3 h reaction; Pd 3d XPS spectra of (b) Pd/CB, (c) Pd/MWCNTs, and (d) Pd/GAC before and after 3 h reaction.

Table 1
Surface area, pore volume, and pore size of bare carbons and carbon-supported Pd catalysts.

Adsorbent	S_{BET} ($m^2\,g^{-1}$)	V_p ($cm^3\,g^{-1}$)	d_p (nm)
CB	184.0	0.94	20.4
MWCNTs	150.0	0.45	12.0
GAC	158.4	0.12	2.7
Pd/CB	174.8	0.32	7.5
Pd/MWCNTs	116.6	0.30	10.2
Pd/GAC	103.7	0.12	4.0

into the 100 mL 0.156 mM 2,4-DCBA solution for a specific time (30 min) without current, then switched on the power supply to start the 2,4-DCBA electrocatalytic dechlorination. As a comparison, 100 mL 0.156 mM 2,4-DCBA solution and the Ni foam electrode were added into the cell for 30 min before the addition of the carbon-supported catalyst and switching on the power supply.

2.5. Analysis methods

The concentrations of 2,4-DCBA, CBA, and BA in the filtered aqueous samples were analyzed by SHI-MADZU HPLC with an Agilent TC-C18 column (150 × 4.6 mm) at 236 nm. The mobile phase was 60:40 (v/v) mixture of methanol: 0.2% H_3PO_4 solution, and the flow rate was 1 mL min^{-1}. The aqueous Cl^- concentration was measured by ion chromatography (Metrohm 883 Basic IC plus). The concentration of the aqueous Pd was measured by ICP-MS (Thermo 6300).

The morphological characteristics of these movable catalysts were observed by scanning electron microscope (SEM, Supra55, Zeiss, Germany) and transmission electron microscopy (TEM, JEM-1230, JEOL, Japan). TEM coupled energy-dispersive X-ray spectroscopy (EDS) was applied to obtain the elements distribution of the catalysts. The chemical compositions and states were detected by X-ray diffraction (XRD, X'pert PRO analytical B.V., Netherlands) and X-ray photoelectron spectroscopy (XPS, Escalab 250 xi, Thermo Fisher Scientific, UK), respectively. The surface area, pore size, and pore volume were measured by Brunauer–Emmett–Teller N_2 adsorption-desorption isotherms (BET, 3H-2000PS2, Bershide Instrument, China). Cyclic voltammetry (CV) and linear sweep voltammetry (LSV) were carried out by an Electrochemical Workstation (SDPTOP Company, EC6800) to study the electrochemical activity of these movable catalysts, with a Ag/AgCl (in 3.0 KCl solution) electrode and a platinum electrode as the reference electrode and the counter electrode, respectively.

3. Results and discussion

3.1. Characterization of the catalysts

The morphologies of Pd/CB, Pd/MWCNTs, and Pd/GAC were firstly analyzed by TEM with the same magnification. Compared with bare carbons (Fig. 1a–c), small Pd nanoparticles (~5 nm) were observed to be dispersedly supported on CB (Fig. 1d) and MWCNTs (Fig. 1e), while large and aggregated Pd particles were found on the surface of GAC

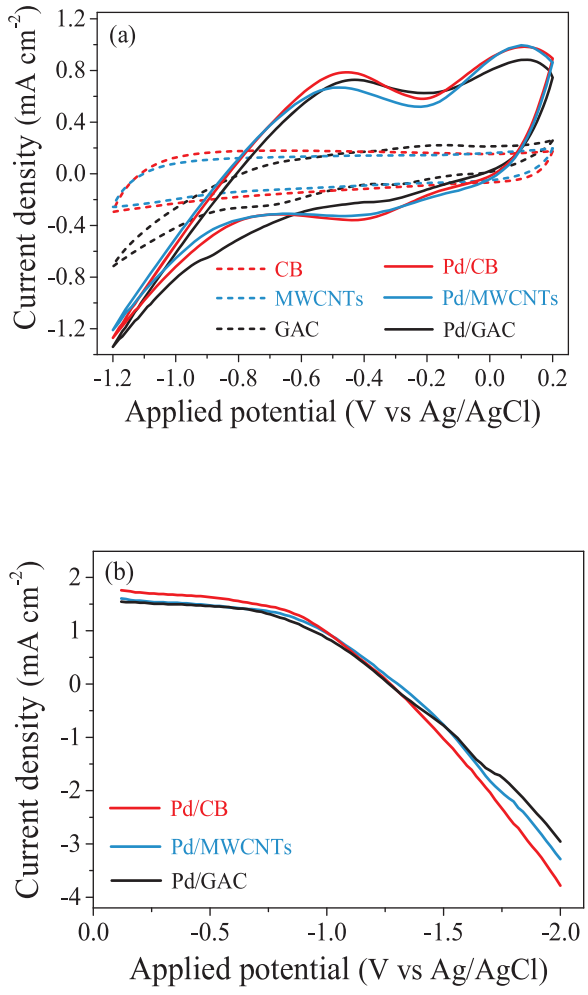

Fig. 4. (a) Cyclic voltammogram (CV) curves of CB, MWCNTs, GAC, Pd/CB, Pd/MWCNTs, and Pd/GAC; (b) Linear sweep voltammogram (LSV) curves of Pd/CB, Pd/MWCNTs, and Pd/GAC moveable catalysts.

(Fig. 1f). Moreover, the size and distribution of these supported particles were almost not changed after 3 h reaction, which indicated the stability of these materials. SEM images (Fig. S1) also show that the CB and MWCNTs were nanoscale spherical particles and interwined structure, respectively, and the deposition of Pd on the surface did not change their structure. While GAC was a much larger structure with pores, and clusters were observed after the deposition of Pd. TEM-EDS mapping, HRTEM, and SADE pattern were further performed to analyze the element and structure of these supported particles. As shown in Fig. 2, the TEM-EDS mapping results confirmed the presence of Pd, and clearly showed that the Pd nanoparticles were well distributed on CB and MWNCTs supports, but aggregated on GAC support. Most of the lattice spacing of Pd/CB, Pd/MWCNTs, and Pd/GAC were found to be around 0.225 nm in their HRTEM images (Fig. S2a–c), matching well with the (111) atomic planes of the face-centered-cubic Pd. Moreover, the SADE pattern of Pd/CB, Pd/MWCNTs, and Pd/GAC indicated the presence of Pd nano-crystallite (Fig. S2d–f), and other atomic planes (200, 220, and 311) were also observed, which was consistent with the results of XRD spectra as described below.

Fig. 2a shows the XRD patterns of the main components and crystalline scattering domain size of Pd/CB, Pd/MWCNTs, and Pd/GAC catalysts. The peak at $2\theta = 24.9^{\circ}$ corresponded with the carbon (003) atomic plane was observed in the spectra of Pd/CB carbon, and the peak at $2\theta = 26.1^{\circ}$ assigned to carbon (002) atomic plane was observed in the spectra of Pd/MWCTNs and Pd/GAC. To some extent, the crystallinity of GAC was better than MWCNTs and CB. Similar typical peaks of Pd were observed in different carbons supported Pd catalysts, which suggested the carbon supports did not change the chemical structure of Pd catalyst that synthesized via the same methods. The stronge peaks at $2\theta = 40.1^{\circ}$ was corresponded to the (111) atomic plane of face-centered-cubic of Pd, while the relatively poor peaks at $2\theta = 46.7^{\circ}$, 68.1°, and 82.1° was corresponded to the typical sharp diffraction of (200), (220), and (311) atomic planes, respectively (JCPDS File No. 87-0641). Notably, the XRD spectra of the materials were almost not changed after reaction, which further suggested the good stability of the moveable carbon-supported catalysts.

The surface Pd species of Pd/CB, Pd/MWCNTs, and Pd/GAC was further investigated by XPS analysis (Fig. 3b–3d). The Pd 3d spectrum exhibited two pairs of spin-orbit components, and the typical binding energy of Pd(0) peaks (334.6 eV) confirmed Pd deposition onto the surface of carbon supports and in agreement with previous studies [41,42]. The higher binding energy miner spin-orbit component pair deduced the presence of Pd(2+) with a lower electron density, which could be assigned to PdO species [43]. More Pd(0) species was observed on the surface of the materials after reaction according to the XPS spectra, indicated the surface Pd(2+) was reduced to Pd(0) during the electrolysis, and the materials maintained the catalytic ability.

BET-N_2 surface area (S_{BET}) analyzer was used to measure the specific surface areas of these catalysts (Table 1). The specific surface area of fine nanoscale CB particles was higher than those of MWCNTs and GAC. The specific surface area of Pd/CB was 174.8 $m^2 g^{-1}$, which was 1.5 and 1.7 times higher than that of Pd/MWCNTs (116.6 $m^2 g^{-1}$) and Pd/GAC (103.7 $m^2 g^{-1}$), respectively. In addition, the total pore volume (V_p) of Pd/CB, Pd/MWCNTs, and Pd/GAC was 0.32, 0.30, and 0.12 $cm^3 g^{-1}$, respectively. And pore diameter (d_p) of Pd/CB, Pd/MWCNTs and Pd/GAC was 7.5, 10.2, and 4.0 nm, respectively.

Since atomic H^* adsorbed on the Pd catalyst was considered as the most reactive species in the electrocatalytic dechlorination [44], CV and LSV characterizations were performed to study the catalytic ability of these carbon supported catalysts. As shown in Fig. 4a, no obvious redox peak was observed in the CVs of bare carbon supports, and the difference range from −1.2 V to −0.8 V of GAC was probably attributed to the impurities (e.g. aluminium) as shown in the EDS spectra (Fig. S4). However, after the deposition of Pd catalyst, both H_2 oxidation peak and atomic H^* oxidation peak were observed at −0.45 V and 0.1 V, respectively [7]. The atomic H^* peak of Pd/CB was similar with that of Pd/MWCNTs, which were both slightly higher than that of Pd/GAC, indicated the stronger reactivity of Pd/BC and Pd/MWCNTs than Pd/GAC. The LSV (Fig. 4b) shows the overpotentials of Pd/CB, Pd/MWCNTs, and Pd/GAC were before −0.8 V and very closed to each other.

3.2. Electrocatalytic dechlorination of 2,4-DCBA

The electrocatalytic dechlorination of 2,4-DCBA by Pd/CB, Pd/MWCNTs, and Pd/GAC under the same experimental conditions were investigated. The error bars of 2,4-DCBA dechlorination by each carbon supported Pd were small (Fig. 5). Hence, both the characterizations and reactivity tests indicated the reproducibility of the supported catalyst in this study. As shown in Fig. 5a, approximately 20% and 10% of 2,4-DCBA was quickly removed in several minutes by Pd/BC and Pd/MWCNTs, respectively, which was because of the adsorption capacity of these carbon supports, considering almost no intermediates was detected (Fig. 5b and c). However, there was a plateau after this fast decrease, one of the possible reasons was that the adsorption of 2,4-DCBA by these carbon supports was significantly inhibited under constant current, which would be discussed later in this paper. Another important reason was because of the activation stage of Pd catalyst [12]. Besides the hydrogen evolution (the quike recombination of atomic H^* to evolved H_2), the atomic H^* produced by the electrolysis would firstly be absorbed and stored into the lattice of Pd (H_{abs}^*), then be adsorbed by the surface of Pd (H_{ads}^*), and the latter was the reactive

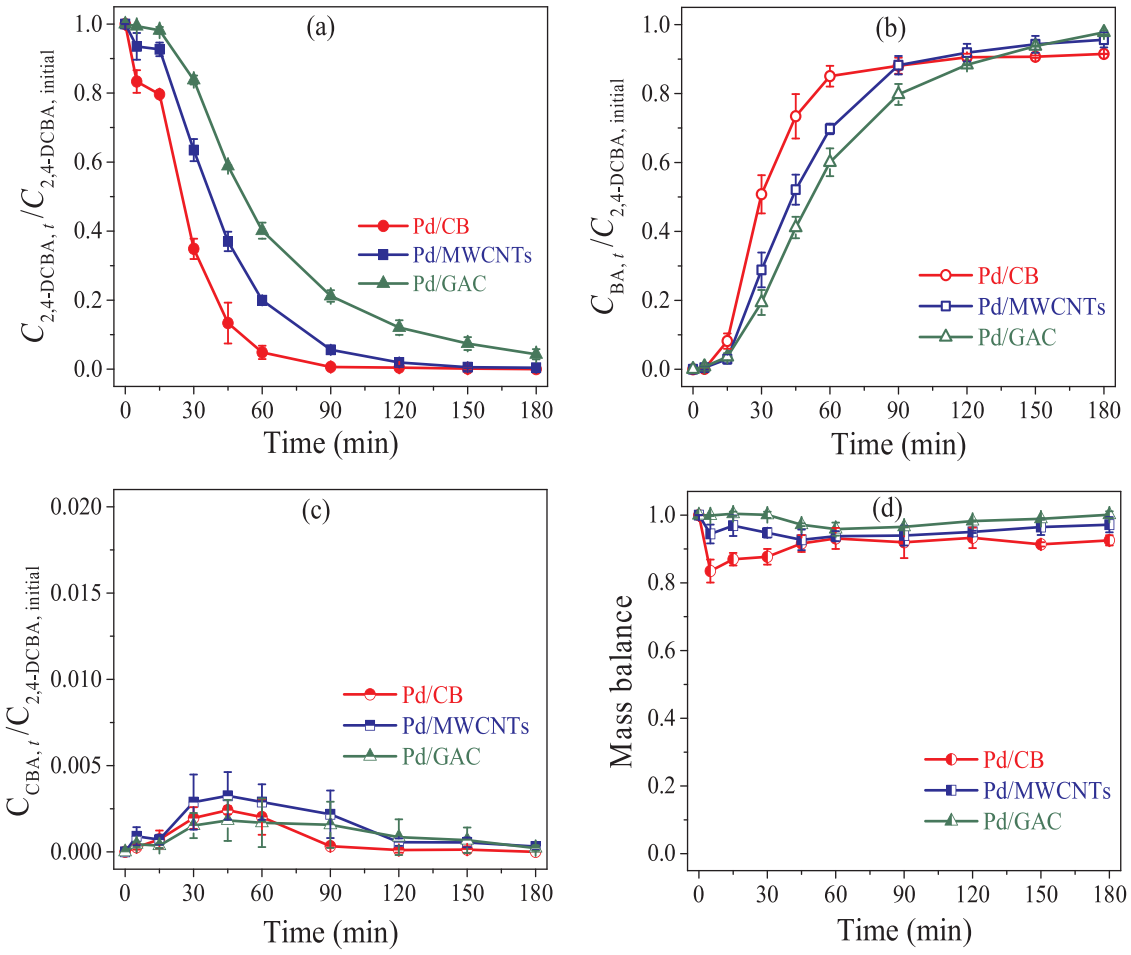

Fig. 5. Comparison of 2,4-DCBA dechlorination by different moveable carbon-supported Pd catalysts; (a) removal of 2,4-DCBA, (b) production efficiency of BA; (c) concentrations of CBA; and (d) mass balance of 2,4-DCBA and its products.

species for hydrodechlorination [45]. Meanwhile, only few dechlorinated products were detected during this period (Fig. 5b). Afterwards, 2,4-DCBA was efficiently removed and BA was quickly generated.

Hence, the data after 15 min was used to be simulated by the pseudo-first-order kinetic to obtain the removal rate of 2,4-DCBA and the generation rate of BA (Fig. S3). Among these moveable catalysts, Pd/CB had the best electrocatalytic performance for 2,4-DCBA dechlorination. The apparent removal rate of 2,4-DCBA by Pd/CB was 0.065 min^{-1}, which was 1.7 and 3.3 times higher than that by Pd/MWCNTs and Pd/GAC, respectively. Almost all the 2,4-DCBA was dechlorinated to BA by Pd/CB within 90 min, while it required 150 min and > 180 min for Pd/MWCNTs and Pd/GAC to completely remove 2,4-DCBA, respectively. Note that almost no CBA was observed during the reaction (Fig. 5c), becuase the dechlorination rate of CBA to BA was much faster than that of 2,4-DCBA to CBA, and the direct dechlorination of 2,4-DCBA to BA might also occur. This result was consistent with the dechlorination of 2,4-dichlorophenol by Pd/Fe nanoparticles and 2,4-DCBA by Pd/MnO_2/Ni foam electrode in our previous studies [45–47]. The experimental Cl^- concentration (Fig. S5) after 3 h reaction was close to the theoretical value, which suggested that the there was no other chlorinated species. The discrepancy between the theoretical and experimental mass balance of 2,4-DCBA and its products (Fig. 5d) was mainly attributed to the adsorption capacity of BA by these catalysts as discussed below. Considering the similar catalytic ability of these carbon supported Pd catalysts obtained from CV and LSV results, we speculated that the adsorption capacity of these catalysts was another factor for the electrocatalytic dechlorination of 2,4-DCBA.

3.3. Adsorption capacities of 2,4-DCBA and BA by different moveable catalysts

The adsorption capacities of 2,4-DCBA and BA by these catalysts without current were investigated, as well as the adsorption of BA with current. The adsorption data of 2,4-DCBA and BA by Pd/CB, Pd/MWCNTs, and Pd/GAC were well fitted by Langmuir isotherm model [48]. As shown in Fig. 6a, the adsorption capacity of 2,4-DCBA by Pd/CB without current was 0.26 mmol g^{-1}, which was 1.6 and 5.2 times higher than that by Pd/MWCNTs and Pd/GAC, respectively. This trend was similar with the adsorption capacity of BA by these moveable catalyst without current (Fig. 6b), and the adsorption capacity of BA was slightly lower than 2,4-DCBA. The lower adsorption of Pd/GAC was because of its lower surface area, pore volume, and pore diameter (Table 1), as well as the lower zeta potential (Fig. S6). The GAC (−26.8 mV) was more negatively charged than CB (−13.6 mV) and MWCNTs (−16.7 mV) at the adsorption experiment condition (pH = 4), which would be repelled the negatively charged 2,4-DCBA and BA. It was reported that the adsorption capacity of chlorinated organics (e.g. 2,4-dichlorophenol, pKa = 7.8) was much higher than non-chlorinated organics (e.g. phenol, pKa = 9.9) when the dissociation of these compounds were limited [47]. However, about 90% of 2,4-DCBA (pKa = 2.8) and 40% of BA (pKa = 4.2) was in the dissociated form with negative charge at pH = 4, which was the reason that the adsorption capacity of 2,4-DCBA was close to BA in this study.

However, in the presence of current, the adsorption capacity of BA

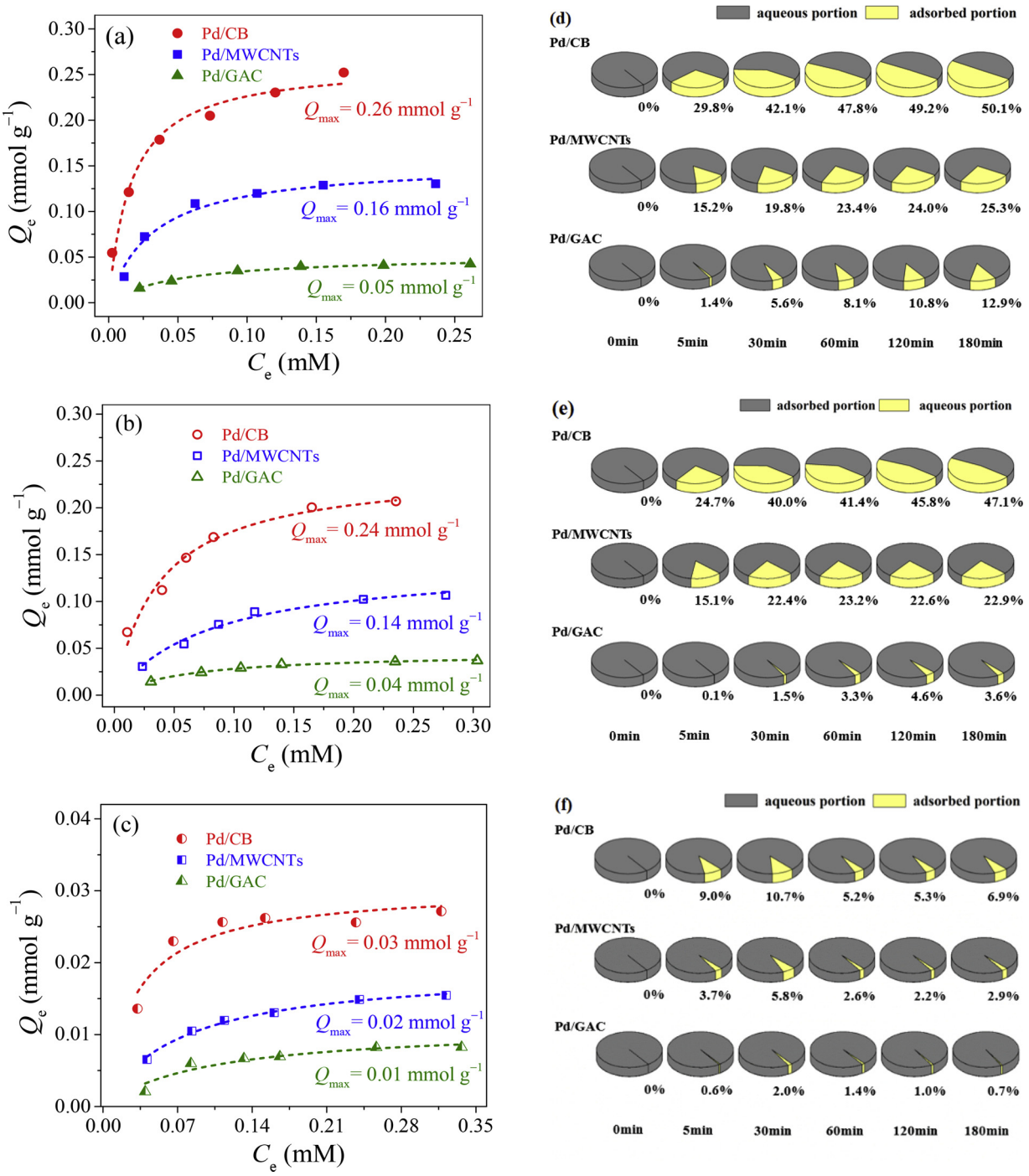

Fig. 6. The adsorption isotherms (well fitted by Langmuir model) of (a) 2,4-DBA without current, (b) BA without current, and (c) BA with current by Pd/CB, Pd/MWCNTs, Pd/GAC moveable catalysts; the adsorption kinetics of (d) 2,4-DBA without current, (e) BA without current, and (f) BA with current by Pd/CB, Pd/MWCNTs, and Pd/GAC moveable catalysts.

by these catalysts was significantly decreased to less than 0.03 mmol g^{-1} (Fig. 6c). Because the pH of the cathodic electrolyte would be gradually increased to basic, and almost all the BA was in the dissociated form with negative charge, which was repelled by the negative charged catalyst. Similar result of 2,4-DCBA adsorption by these catalyst in the presence of current could be expected. Hence, the adsorption of the compounds was limited in this study, which caused the small discrepancy between the theoretical and experimental mass balance (Fig. 5d).

The kinetics of 2,4-DCBA and BA adsorption with the same initial concentration as dechlorination experiments (Fig. 6d–f) were also investigated. The pseudo-first-order model [49] and pseudo-second-order model [50] were used to fit the experimental data, and the results were summarized in Table 2.

$$\text{Pseudo-first-order:} \frac{dq_t}{dt} = k_1(q_e - q_t) \quad (1)$$

$$\text{Pseudo-second-order:} \frac{t}{q_t} = \frac{1}{k_2 q_e^2} + \frac{1}{q_e} t \quad (2)$$

where q_t (mg g^{-1}) and q_e (mg g^{-1}) is the adosprtion capacity at time t and equilibrium, respectively; k_1 (min^{-1}) and k_2 (g mg^{-1} min^{-1}) is the

Table 2
Kinetics of the 2,4-DCBA and BA adsorption by the moveable carbon-supported Pd catalyst without current.

Compounds	Materials	Pseudo-first-order kinetics			Pseudo-second-order kinetics		
		q_e	k_1	R^2	q_e	k_2	R^2
2,4-DCBA	Pd/CB	35.4	0.164	0.952	37.7	0.007	0.990
	Pd/MWCNTs	17.0	0.166	0.902	18.2	0.013	0.962
	Pd/GAC	9.5	0.019	0.984	12.2	0.001	0.992
BA	Pd/CB	20.8	0.135	0.957	22.3	0.009	0.991
	Pd/MWCNTs	10. 9	0.204	0.987	11.4	0.033	0.990
	Pd/GAC	12.2	0.055	0.888	13.6	0.006	0.983

q_e: mg g^{-1}; k_1: min^{-1}; k_2: g mg^{-1} min^{-1}.

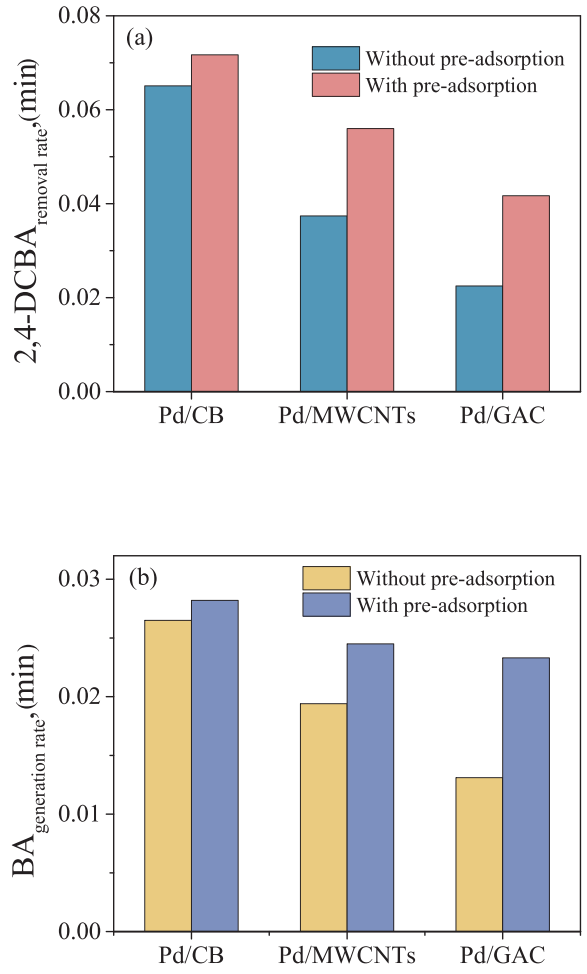

Fig. 7. The (a) removal rate of 2,4-DCBA and (b) generation rate of BA (with or without 30 min pre-adsorption) by Pd/CB, Pd/MWCNTs, and Pd/GAC.

rate constant for the pseudo-first-order and pseudo-second-order model, respectively.

The pseudo-second-order kinetic model (average $R^2 > 0.985$) was observed to better fit the data than pseudo-first-order kinetic model (average $R^2 > 0.945$) in the absence of current. The kinetics of BA adsorption in the presence of current was not studied because the percentages in the BA adsorption with current was decreased after 30 min (Fig. 6f). This phenomenon was attributed to the gradually increased pH of the cathodic electrolyte during electrolysis, and more and more BA (pKa = 4.2) was in the dissociated form with negative charge during the electrolysis, and the decreased adsorption capacity was caused by the electro-repulsion between the negatively charged BA and cathode.

3.4. Effect of the pre-adsorption on the dechlorination of 2,4-DCBA

Since the adsorption of 2,4-DCBA by the Pd/CB, Pd/MWCNTs, and Pd/GAC were expected to be greatly inhibited in the presence of current due to the electro-repulsion between the negatively charged compounds and adsorbent (as previously discussed), a pre-adsorption process with little energy consumption was applied to improve the degradation of 2,4-DCBA, especially the initial dechlorination rate since a proportion of 2,4-DCBA was already adsorbed on the catalyst when the electrolysis started. The effects of a 30 min pre-adsorption on the removal of 2,4-DCBA and the generation of BA by the moveable carbon-supported Pd catalysts were investigated (Fig. S7).

The apparent removal rate of 2,4-DCBA was increased after the pre-adsorption (Fig. 7a). Although the lower initial concentration of 2,4-DCBA (aqueous) would result in the higher apparent rate of 2,4-DCBA, both the pre-adsorbed 2,4-DCBA on the catalyst and the 2,4-DCBA in the solution would be degraded, and the actual dechlorination of 2,4-DCBA with or without pre-adsorption could both be described by the generation of BA in this study. As shown in Fig. 7b, no BA was detected (as well as no CBA was detected) in the first 30 min, only about 6%, 20% and 45% of 2,4-DCBA was adsorbed by the Pd/CB, Pd/MWCNTs, and Pd/GAC catalysts, respectively. While the 2,4-DCBA was not changed without the pre-adsorption (only Ni foam) during the first 30 min. However, more BA was generated and the generation rate of BA was higher in all cases with pre-adsorption than that without pre-adsorption (Fig. S7b and Fig. 7b). The effect of the pre-adsorption on the removal rate of 2,4-DCBA and generation rate of BA by Pd/CB was slight, because the reactivity of Pd/CB was already very high. The enhancement of the dechlorination of 2,4-DCBA by the pre-adsorption process was more obvious for the catalysts (Pd/MWCNTs and Pd/GAC) with relative lower reactivity. These results suggested that the contaminant pre-adsorption onto the catalyst is a promising strategy, which not only to improve the removal rate of the contaminant, but also to shorten the electrolysis process to decrease the energy consumption.

3.5. Stability and reusability of moveable Pd/CB catalyst

Easy loss of catalyst and poor long-term performance were two of the important issues that need to be addressed for the development of electrocatalytic technology. Therefore, in order to investigate the stability and reusability of these moveable catalysts, 10 consecutive experimental cycles (3 h each cycle) were performed to assess the performance of Pd/CB as the represented catalyst in this study. The removal efficiency of 2,4-DCBA and production efficiency of BA could reach to 100% and 93.6% in all cycles (Fig. 8a and b), respectively, and the discrepancy of BA (6%) was attributed to the adsorption of BA by Pd/CB as previously discussed (Figs. 5 and 6). As shown in Fig. 8c, the removal rate of 2,4-DCBA by moveable Pd/CB in 10 cycles was maintained at the same level, and the average rate was $0.067 \pm 0.002\ min^{-1}$. The released Pd from the catalyst to the solution was lower than 0.05% in each cycle (Fig. 8d), it was almost not

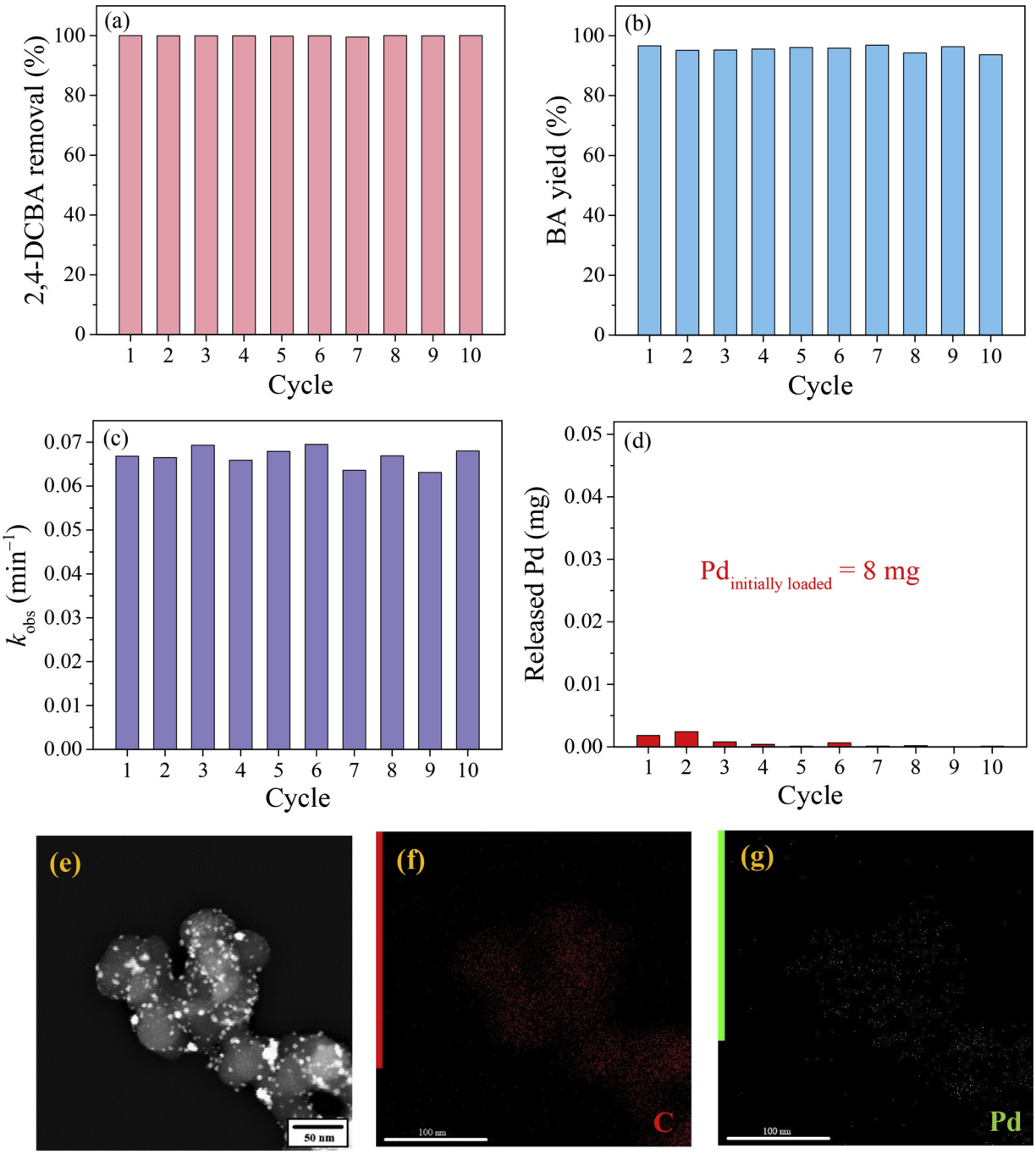

Fig. 8. Stability and reusability of moveable Pd/CB catalyst during 10 consecutive cycles. (a) Removal efficiency of 2,4-DCBA, (b) production of BA, (c) removal rate of 2,4-DCBA, (d) released Pd at the end of each cycle, (e–f) TEM-EDS mapping.

detected in some cycles, the loss of the Pd catalyst could be ignored. Moreover, the morphology of Pd/CB after 10 cycles test was also investigated. Both the TEM image (Fig. S8) was similar as the Pd/CB catalyst before reaction (Fig. 1d) and after 3 h reaction (Fig. 1g), and the EDS mapping (Fig. 8e–f) was also similar as the Pd/CB before reaction (Fig. 2a–c), indicated the morphology and elements of Pd/CB were almost not changed during the reaction. These results clearly suggested the excellent reactivity, stability, and reusability movable of the Pd/CB catalyst, which would be a promising strategy for the degradation of chlorinated contaminant from water.

4. Conclusions

The present study investigated the performance of moveable catalysts (Pd/CB, Pd/MWCNTs, and Pd/GAC) for the removal of 2,4-DCBA. All the moveable carbon-supported catalysts exhibited good reactivity and stability. The moveable Pd/CB catalyst shows the best reactivity for 2,4-DCBA dechlorination, and the adsorption capacity of 2,4-DCBA and BA by CB was also higher than MWCNTs and GAC. The adsorption was greatly inhibited in the presence of current, and pre-adsorption was proved to be another method to improve the dechlorination of 2,4-DCBA. The morphology, loaded Pd distribution and amount, and reactivity of the moveable Pd/CB catalyst was almost not changed after 10 cycles test. All these results suggested that the moveable carbon-

supported Pd catalyst was a promising strategy to address the issues of easy catalyst loss and limited long-term performance of electrocatalytic remediation technology.

Acknowledgment

The authors are grateful to the financial support provided by the National Natural Science Foundation of China (No. 21477108).

Appendix A. Supplementary data

Supplementary material related to this article can be found, in the online version, at doi:https://doi.org/10.1016/j.apcatb.2018.11.052.

References

[1] D.F. Laine, I.F. Cheng, The destruction of organic pollutants under mild reaction conditions: a review, Microchem. J. 85 (2007) 183–193.
[2] R. Weber, Relevance of PCDD/PCDF formation for the evaluation of POPs destruction technologies – Review on current states and assessment gaps, Chemosphere 67 (2007) S109–S117.
[3] A.I. Tsyganok, I. Yamanaka, K. Otsuka, Dechlorination of chloroaromatics by electrocatalytic reduction over palladium-loaded carbon felt at room temperature, Chemosphere 39 (1999) 1819–1831.
[4] Y.Z. Liu, R. Mao, Y.T. Tong, H.C. Lan, G. Zhang, H.J. Liu, J.H. Qu, Reductive dechlorination of trichloroacetic acid (TCAA) by electrochemical process over Pd-In/Al2O3 catalyst, Electrochim. Acta 232 (2017) 13–21.
[5] S. Rondinini, P.R. Mussini, M. Specchia, A. Vertova, The electrocatalytic performance of sliver in the reductive dehalogenation of bromophenols, J. Electrochem. Soc. 148 (2001) D102–D107.
[6] M.C. Li, D.D. Bao, C.A. Ma, Studies on electrochemical hydrodebromination mechanism of 2,5-dibromobenzoic acid on Ag electrode by in situ FTIR spectroscopy, Electrochim. Acta 56 (2011) 4100–4104.
[7] G.M. Jiang, M.N. Lan, Z.Y. Zhang, X.S. Lv, Z.M. Lou, X.H. Xu, F. Dong, S. Zhang, Identification of active hydrogen species on palladium nanoparticles for an enhanced electrocatalytic hydrodechlorination of 2,4-dichlorophenol in water, Environ. Sci. Technol. 51 (2017) 7599–7605.
[8] Z.R. Sun, X.F. Wei, Y.B. Han, S. Tong, X. Hu, Complete dechlorination of 2,4-dichlorophenol in aqueous solution on palladium/polymeric pyrrole-cetyl trimethyl ammonium bromide/foam-nickel composite electrode, J. Hazard. Mater. 244 (2013) 287–294.
[9] Q.D. Huang, J.F. Rusling, Formal reduction potentials and redox chemistry of polyhalogenated biphenyls in a bicontinuous microemulsion, Environ. Sci. Technol. 29 (1995) 98–103.
[10] D. Voglar, D. Lestan, Electrochemical treatment of spent solution after EDTA-based soil washing, Water Res. 46 (2012) 1999–2008.
[11] A.Z. Li, X. Zhao, Y.N. Hou, H.J. Liu, L.Y. Wu, J.H. Qu, The electrocatalytic dechlorination of chloroacetic acids at electrodeposited Pd/Fe-modified carbon paper electrode, Appl. Catal. B 111 (2012) 628–635.
[12] C. Sun, S.A. Baig, Z.M. Lou, J. Zhu, Z.X. Wang, X. Li, J.H. Wu, Y.F. Zhang, X.H. Xu, Electrocatalytic dechlorination of 2,4-dichlorophenoxyacetic acid using nanosized titanium nitride doped palladium/nickel foam electrodes in aqueous solutions, Appl. Catal. B (2014) 38–47 158–159.
[13] R. Mao, N. Li, H.C. Lan, X. Zhao, H.J. Liu, J.H. Qu, M. Sun, Dechlorination of trichloroacetic acid using a noble metal-free graphene-Cu foam electrode via direct cathodic reduction and atomic H*, Environ. Sci. Technol. 50 (2016) 3829–3837.
[14] Z.Q. He, L.Y. Zhan, Q. Wang, S. Song, J.M. Chen, K.R. Zhu, X.H. Xu, W.P. Liu, Increasing the activity and stability of chemi-deposited palladium catalysts on nickel foam substrate by electrochemical deposition of a middle coationg of silver, Sep. Purif. Technol. 80 (2011) 526–532.
[15] K.R. Zhu, C. Sun, H. Chen, S.A. Baig, T.T. Sheng, X.H. Xu, Enhanced catalytic hydrodechlorination of 2,4-dichlorophenoxyacetic acid by nanoscale zero valent iron with electrochemical technique using a palladium/nickel foam electrode, Chem. Eng. J. 223 (2013) 192–199.
[16] C. Zhang, Y.H. Jiang, Y.L. Li, Z.X. Hu, L. Zhou, M.H. Zhou, Three-dimensional electrochemical process for wastewater treatment: a general review, Chem. Eng. J. 228 (2013) 455–467.
[17] X.P. Zhu, J.R. Ni, X. Xing, H.N. Li, Y. Jiang, Synergies between electrochemical oxidation and activated carbon adsorption in three-dimensional boron-doped diamond anode system, Electrochim. Acta 56 (2011) 1270–1274.
[18] T.C. An, X.H. Zhu, Y. Xiong, Feasibility study of photoelectrochemical degradation of methylene blue with three-dimensional electrode-photocatalytic reactor, Chemosphere 46 (2002) 897–903.
[19] J. Xu, Z. Cao, X. Liu, H. Zhao, X. Xiao, J.P. Wu, X.H. Xu, J.L. Zhou, Preparation of functionalized Pd/Fe-Fe3O4@MWCNTs nanomaterials for aqueous 2,4-dichlorophenol removal: interactions, influence factors, and kinetics, J. Hazard. Mater. 317 (2016) 656–666.
[20] B. Shen, X.H. Wen, X. Huang, Enhanced removal performance of estriol by a three-dimensional electrode reactor, Chem. Eng. J. 327 (2017) 597–607.
[21] Y. Yavuz, R. Shahbazi, Anodic oxidation of reactive black 5 dye using boron doped diamond anodes in a bipolar trickle tower reactor, Sep. Purif. Technol. 85 (2012) 130–136.
[22] G. Yuan, M.A. Keane, Liquid phase catalytic hydrodechlorination of 2,4-dichlorophenol over carbon supported palladium: an evaluation of transport limitations, Chem. Eng. Sci. 58 (2003) 257–267.
[23] Y. Tian, Z. Wei, K.H. Zhang, S. Peng, X. Zhang, W.M. Liu, K. Chu, Three-dimensional phosphorus-doped graphene as an efficient metal-free electrocatalyst for electrochemical sensing, Sens. Actuators B Chem. 241 (2017) 584–591.
[24] Z.S. Li, Z.S. Liu, B.L. Li, Z.H. Liu, D.H. Li, H.Q. Wang, Q.Y. Li, Hollow hemisphere-shaped macroporous graphene/tungsten carbide/platinum nanocomposite as an efficient electrocatalyst for the oxygen reduction reaction, Electrochim. Acta 221 (2016) 31–40.
[25] J.O.'M. Bockris, J. Kim, Effect of contact resistance between particles on the current distribution in a packed bed electrode, J. Appl. Electrochem. 27 (1997) 890–901.
[26] H.Z. Ma, B. Wang, Electrochemical pilot-scale plant for oil field produced wastewater by M/C/Fe electrodes for injection, J. Hazard. Mater. 132 (2006) 237–243.
[27] W. Can, H.Y. Kun, Z. Qing, J. Min, Treatment of secondary effluent using a three-dimensional electrodesystem: COD removal, biotoxicity assessment, and disinfection effects, Chem. Eng. J. 243 (2014) 1–6.
[28] B.P. Chaplin, M. Reinhard, W.F. Schneider, C. Schuth, J.R. Shapley, T.J. Strathmann, C.J. Werth, Critical review of Pd-based catalytic treatment of priority contaminants in water, Environ. Sci. Technol. 46 (2012) 3655–3670.
[29] M. Shao, Palladium-based electrocatalysts for hydrogen oxidation and oxygen reduction reactions, J. Power Sources 196 (2011) 2433–2444.
[30] S. Wang, B. Yang, T.T. Zhang, G. Yu, S.B. Deng, J. Huang, Catalytic hydrodechlorination of 4-chlorophenol in an aqueous solution with Pd/Ni catalyst and formic acid, Ind. Eng. Chem. Res. 49 (2010) 4561–4565.
[31] N.S. Babu, N. Lingaiah, J.V. Kumar, P.S.S. Prasad, Studies on alumina supported Pd-Fe bimetallic catalysts prepared by deposition-precipitation method for hydrodechlorination of chlorobenzene, Appl. Catal. A Gen. 367 (2009) 70–76.
[32] J. Xu, L.S. Tan, S.A. Baig, D.L. Wu, X.S. Lv, X.H. Xu, Dechlorination of 2,4-dichlorophenol by nanoscale magnetic Pd/Fe particles: effects of pH, temperature, common dissolved ions and humic acid, Chem. Eng. J. 231 (2013) 26–35.
[33] J. Xu, J. Tang, S.A. Baig, X.S. Lv, X.H. Xu, Enhanced dechlorination of 2,4-dichlorophenol by Pd/Fe-Fe3O4 nanocomposites, J. Hazard. Mater. (2013) 628–636 244–245.
[34] T. Li, J.H. Farrell, Reductive dechlorination of trichloroethene and carbon tetrachloride using iron and palladized-iron cathodes, Environ. Sci. Technol. 34 (2000) 173–179.
[35] S.A. Adebusoye, M. Miletto, Characterization of multiple chlorobenzoic acid-degrading organisms from pristine and contaminated systems: mineralization of 2,4-dichlorobenzoic acid, Bioresour. Technol. 102 (2011) 3041–3048.
[36] Y.C. Zhao, Z. Ning, J.N. Tian, H.W. Wang, X.Y. Liang, S.L. Nie, Y. Yu, X.X. Li, Hydrogen generation by hydrolysis of alkaline NaBH4 solution on Co-Mo-Pd-B amorphous catalyst with efficient catalytic properties, J. Power Sources 27 (2012) 120–126.
[37] X.L. Cui, W. Zuo, M. Tian, Z.P. Dong, J.T. Ma, Highly efficient and recyclable Ni MOF-derived N-doped magnetic mesoporous carbon-supported palladium catalysts for the hydrodechlorination of chlorophenols, J. Mol. Catal. A Chem. 423 (2016) 386–392.
[38] J.S. Zhou, Z.M. Lou, J. Xu, X.X. Zhou, K.L. Yang, X.Y. Gao, Y.L. Zhang, X.H. Xu, Enhanced electrocatalytic dechlorination by dispersed and moveable activated carbon supported palladium catalyst, Chem. Eng. J. 358 (2019) 1176–1185.
[39] C.W. Xu, L.Q. Cheng, P.K. Shen, Y.L. Liu, Methanol and ethanol electrooxidation on Pt and Pd supported on carbon microspheres in alkaline media, Electrochem. Commun. 9 (2007) 997–1001.
[40] W.J. Xie, S.H. Yuan, X.H. Mao, W. Hu, P. Liao, M. Tong, A.N. Alshaulabkeh, Electrocatalytic activity of Pd-loaded Ti/TiO2 nanotubes cathode for TCE reduction in groundwater, Water Res. 47 (2013) 3573–3582.
[41] R. Muftikan, K. Nebesny, Q. Fernando, N. Korte, X-ray photoelectron spectra of the palladium-iron bimetallic surface used for the rapid dechlorination of chlorinated organic environmental contaminants, Environ. Sci. Technol. 30 (1996) 3593–3596.
[42] X. Zhao, A.Z. Li, R. Mao, H.J. Liu, J.H. Qu, Electrochemical removal of haloacetic acids in a three-dimensional electrochemical reactor with Pd-GAC particles as fixed filler and Pd-modified carbon paper as cathode, Water Res. 51 (2014) 134–143.
[43] I.G. Casella, M. Contursi, Pulsed electrodeposition of nickel/palladium globular particles from an alkaline gluconate bath. An electrochemical, XPS and SEM investigation, J. Electroanal. Chem. 692 (2013) 80–86.
[44] C. Sun, Z.M. Lou, Y. Liu, R.Q. Fu, X.X. Zhou, Z. Zhang, S.A. Baig, X.H. Xu, Influence of environmental factors on the electrocatalytic dechlorination of 2,4-dichlorophenoxyacetic acid on nTiN doped Pd/Ni foam electrode, Chem. Eng. J. 281 (2015) 183–191.
[45] Z.M. Lou, J.S. Zhou, M. Sun, J. Xu, K.L. Yang, D. Lv, Y.P. Zhao, X.H. Xu, MnO2 enhances electrocatalytic hydrodechlorination by Pd/Ni foam electrodes and reduces Pd needs, Chem. Eng. J. 352 (2018) 549–557.
[46] J. Xu, X. Liu, G.V. Lowry, Z. Cao, H. Zhao, J.L. Zhou, X.H. Xu, Dechlorination mechanism of 2,4-dichlorophenol by magnetic MWCNTs supported Pd/Fe nanohybrids: rapid adsorption, gradual dechlorination, and desorption of phenol, ACS Appl. Mater. Inter. 8 (2016) 7333–7342.
[47] J. Xu, T.T. Sheng, Y.J. Hu, S.A. Baig, X.S. Lv, X.H. Xu, Adsorption-dechlorination of 2,4-dichlorophenol using two specified MWCNTs-stabilized Pd/Fe nanocomposites, Chem. Eng. J. 219 (2013) 162–173.
[48] A.K. Mishra, S. Ramaprabhu, Magnetite decorated multiwalled carbon nanotube based supercapacitor, J. Phys. Chem. C 114 (2010) 2583–2590.
[49] M. Ozacar, I.A. Sengil, Adsorption of reactive dyes on calcined alunite from aqueous solutions, J. Hazard. Mater. B98 (2003) 211–224.
[50] Y.S. Ho, G. McKay, Kinetic model for lead(II) sorption on to peat, Adsorp. Sci. Technol. 16 (1998) 243–255.